

## Methanol-tolerant PdPt/C alloy catalyst for oxygen electro-reduction reaction

Ji Bong Joo\*, You Jung Kim\*, Wooyoung Kim\*, Nam Dong Kim\*, Pil Kim\*\*, Younghun Kim\*\*\*, and Jongheop Yi\*†

\*School of Chemical and Biological Engineering, Institute of Chemical Processes, Seoul National University, Shinlim-dong, Gwanak-gu, Seoul 151-744, Korea

\*\*School of Chemical Engineering & Specialized Graduate School of Hydrogen and Fuel Cell Engineering, Chonbuk National University, Deokjin dong, Deokjin-gu, Jeonju 561-756, Korea

\*\*\*Department of Chemical Engineering, Kwangwoon University, Wolgye-dong, Nowon-gu, Seoul 139-701, Korea  
(Received 4 June 2007 • accepted 21 November 2007)

**Abstract**—A carbon-supported Pd-based PdPt catalyst (PdPt/C) with a small amount of Pt was prepared by borohydride reduction method and its activity in the oxygen electro-reduction reaction (ORR) was investigated in acidic conditions both with and without methanol. For comparison, carbon-supported Pt (Pt/C) and Pd (Pd/C) catalysts were prepared and the ORR activities were compared. Results revealed that the PdPt/C catalyst showed slightly lower ORR activity in terms of onset potential of oxygen reduction than Pt/C catalyst in 0.1 M HClO<sub>4</sub>. However, PdPt/C catalyst exhibited enhanced activity toward selective ORR with methanol-tolerant characteristics in 0.1 M HClO<sub>4</sub> in the presence of methanol. The PdPt/C catalyst prepared here is suitable for use as a cathodic electrocatalyst in direct alcohol fuel cells after addition of small amount of expensive Pt metal.

Key words: Electrocatalyst, PdPt Alloy, Oxygen Reduction, Methanol Tolerant, Fuel Cell

### INTRODUCTION

In the last decades, Pt-based catalysts have attracted a great deal of attention due to their promising applications, particularly as the electrode catalyst for low-temperature fuel cells and considerable progress has been achieved [1-8]. Although Pt-based catalysts have excellent electrocatalytic activity in both methanol electro-oxidation and oxygen electro-reduction, some obstacles still remain for the commercialization of fuel cells, such as the high cost of Pt and the reduction of the cell performance that originates from the mixed potential by liquid fuel crossover from anode to cathode [9,10]. Consequently, the major issues facing low temperature fuel cells are the costdown of electrode and finding a new selective oxygen-reduction catalyst on cathode electrode. Therefore, many research groups have attempted to develop new low-cost electrocatalysts that could not only reduce expensive Pt-based catalysts, but selectively catalyze oxygen electro-reduction with strong tolerance to methanol [11,12].

Recently, two approaches have been extensively investigated to reduce Pt cost in fuel cells: the first one is to explore non-noble metal catalysts, and the second is to reduce the Pt loading [13,14]. In the first approach, non-noble catalysts, such as metal carbide, transition metal chalcogenides, and heat-treated transition metal macrocycles, showed electrocatalytic activity toward ORR with high methanol tolerance [15-19]. However, their catalytic activities were still insufficient for the practical fuel cell operation and their stability was limited for long-term operation. The second approach is Pt-metal alloying [20,21]. Some results on the use of Pt-metal alloys have been reported for catalytic activity enhancement and fuel cell performance improvement. However, the high cost of a catalyst, the short lifetime of a low Pt-loading catalyst and the severe decrease in fuel cell performance due to the mixed potential of simultaneous

reactions of ORR and methanol electro-oxidation on the cathode are still serious obstacles for practical applications.

As an alternative way, Palladium (Pd)-based alloy catalysts were investigated as a fuel cell catalyst. Pd is less expensive and more abundant (Pd is at least 50 times more available) than Pt [22,23]. Recently, it has been reported that Pd has considerable catalytic activity toward hydrogen oxidation (HOR) and ORR, and no significant activity with CO and methanol [24-26]. In addition, it has been known that Pd-based electrocatalysts exhibited considerable performance in practical low temperature fuel cells. Especially, Pd-based PdPt/C catalyst with a Pd : Pt atomic ratio of 19 : 1 was successfully applied for anode electrode in polymer electrolyte fuel cell (PEMFC) [27]. Pd is also a potential electrocatalyst for cathodic oxygen electro-reduction in direct methanol fuel cells (DMFC). It is reported that Pd has a direct 4-electron oxygen reduction pathway, which is a similar property to Pt and Pd showing inactivity in methanol electro-oxidation [28].

The ORR activity of Pd-based electrocatalysts was enhanced by alloying with another transition metal such as Pt, Au, Co or Fe [29-34]. However, the ORR overpotential of Pd catalysts was still higher than that of Pt. Thus, for practical use in direct methanol fuel cells, it is necessary to develop cost-effective Pd-based alloy catalysts that have enhanced activity toward selective ORR in the presence of methanol.

In this work, we prepared carbon-supported Pd-based PdPt alloy catalysts with small Pt content by sodium borohydride reduction. The prepared PdPt/C catalyst was characterized by XRD, TEM and electrochemical methods. The ORR activity of PdPt/C catalyst was investigated by using linear sweep methods in an acidic electrolyte both with and without methanol.

### EXPERIMENTAL

Carbon-supported PdPt, Pd and Pt catalysts were prepared by

†To whom correspondence should be addressed.  
E-mail: jyji@snu.ac.kr

NaBH<sub>4</sub> reduction. Pd precursor (PdCl<sub>2</sub>, Aldrich) and Pt precursor (H<sub>2</sub>PtCl<sub>6</sub>, Acrose) were dissolved in deionized water, and the carbon support (Vulcan XC-72, Carbot Corp.) was well dispersed with an ultrasonicator for 30 min. As a reducing agent, aqueous 0.2 M NaBH<sub>4</sub> was added dropwise to the parent solution, and the mixture was kept in ambient condition for 3 hr with vigorous stirring. The above mixture was filtered and washed with copious amounts of water to obtain the PdPt/C catalyst. The metal content was maintained at 20 wt% in the catalyst with a 5 : 1 weight ratio of Pd/Pt. For comparison purposes, 20 wt% carbon-supported Pd (Pd/C) and Pt catalyst (Pt/C) were prepared by the same method.

X-ray diffraction patterns of the prepared catalysts were recorded on an M18HF-SRA diffractometer (MAC science) using CuK $\alpha$  radiation. Morphologies and metal dispersions of the prepared catalysts were observed by transmission electron microscopy (TEM, Jeol JEM-3010).

Electrochemical properties of the prepared catalysts were investigated by conventional three-electrode system with EG&G 263A potentiostat. A saturated calomel electrode (SCE) and a platinum gauge were used as the reference electrode and the counter electrode, respectively. The working electrode was prepared by coating catalyst ink on disk-type graphite. Cyclic voltammograms (CVs) of the prepared catalysts were obtained at ambient temperature in 0.1 M HClO<sub>4</sub> solution in the range of -0.25 to 1 V (vs. SCE) at 20 mV/s. The ORR activities of the prepared catalysts were evaluated in O<sub>2</sub>-saturated 0.1 M HClO<sub>4</sub> with and without 0.5 M CH<sub>3</sub>OH by using a rotating glassy carbon disk electrode (RDE 616, Princeton Applied Research) at ambient temperature. Slow sweep voltammograms were recorded between 0.8 and -0.2 V (vs. SCE) at 5 mV/s.

## RESULTS AND DISCUSSION

The Pt and Pd contents of the prepared Pt/C, Pd/C and PdPt/C catalysts were determined by FE-SEM EDS. The average composition of Pd and Pt in PdPt/C catalyst was a weight ratio of 79 to 21. The structure and crystalline phase of the prepared catalysts were investigated by XRD, as shown in Fig. 1. Broad peaks at about 2 $\theta$  = 25° were observed in all catalysts due to the (002) diffraction plane

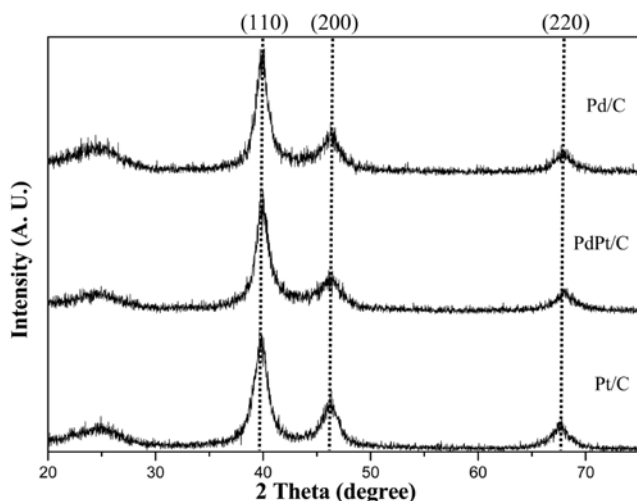


Fig. 1. XRD patterns of the prepared catalysts.

of the hexagonal structure of the carbon support, which implied that support material of carbon (Vulcan XC-72R, Carbot) has partially crystalline properties. The prepared catalysts showed (110), (200) and (220) diffraction peaks at about 39°, 46° and 68°, which indicated that Pt, Pd and PdPt alloy nanoparticles with typical face-centered cubic (fcc) structure were formed on the carbon support. The 2 $\theta$  values of the diffraction peaks were seen at the almost identical positions in all catalysts. Since the atomic radii of Pt and Pd are almost same, diffraction peaks of Pt, Pd and PdPt alloy catalysts were observed at the same 2 $\theta$  position as seen in Fig. 1. Average crystallite sizes of Pt, Pd and PdPt alloy nanoparticles were calculated by using the Scherrer formula based on the (220) peak because the (220) peak is isolated from other carbon-related diffraction peaks.

$$D = \frac{0.9\lambda}{B \cos \theta_b}$$

Where D is an average crystallite size,  $\lambda$  is the X-ray wavelength (CuK $\alpha$  = 1.54 Å), B is the full width half maximum (FWHM), and  $\theta_b$  values represent (220) peak positions. In addition, surface areas (S) of Pt, Pd and PdPt nanoparticles were calculated from the crystallite size by using the following equation:

$$S = \frac{6000}{\rho d}$$

Where S is the surface area (m<sup>2</sup>/g), d is the average crystallite size (nm), and  $\rho$  represents densities of Pd (12.3 g/cm<sup>3</sup>), Pt (21.4 g/cm<sup>3</sup>) and PdPt alloy (13.82 g/cm<sup>3</sup>). The density of PdPt/C catalyst was calculated from the following equation, assuming that all Pt and Pd atoms are homogeneously alloyed.

$$\rho_{PdPt} = \rho_{Pd} \times X_{Pd} + \rho_{Pt} \times X_{Pt}$$

Where  $\rho_{PdPt}$ ,  $\rho_{Pd}$  and  $\rho_{Pt}$  are densities of PdPt alloy, Pd and Pt, respectively.  $X_{Pd}$  and  $X_{Pt}$  are weight ratios of Pd and Pt in PdPt/C catalyst, respectively. The crystallite size and surface area are summarized in Table 1.

Morphologies and metal dispersion were examined by TEM analysis (Fig. 2). Pt, Pd and PdPt nanoparticles were well dispersed on the spherical carbon support. Among three catalysts, Pt/C had the smallest Pt particle size with high metal dispersion, while Pd/C catalyst had the largest Pd nanoparticle. The average particle size was estimated by measuring particles using randomly distributed 100 particles in TEM images. Metal nanoparticle sizes of Pt/C, Pd/C and PdPt/C were estimated to be a ca. 4.6, 5.2 and 4.8 nm, respectively. These estimated metal sizes from TEM were consistent with those estimated from XRD results.

Electrochemical properties of the prepared Pt/C, Pd/C and PdPt/C catalysts were investigated by cyclic voltammetry in acidic conditions (0.1 M HClO<sub>4</sub>). Fig. 3(a) shows the cyclic voltammograms

Table 1. Average crystallite sizes calculated from the (220) diffraction plane using the Scherrer equation and surface areas of Pt, Pd and PdPt alloy crystallites

	$D_{XRD}$ (nm)	$S_{XRD}$ (m <sup>2</sup> /g)
Pt/C	4.3	64
PdPt/C	4.5	97
Pd/C	4.9	97

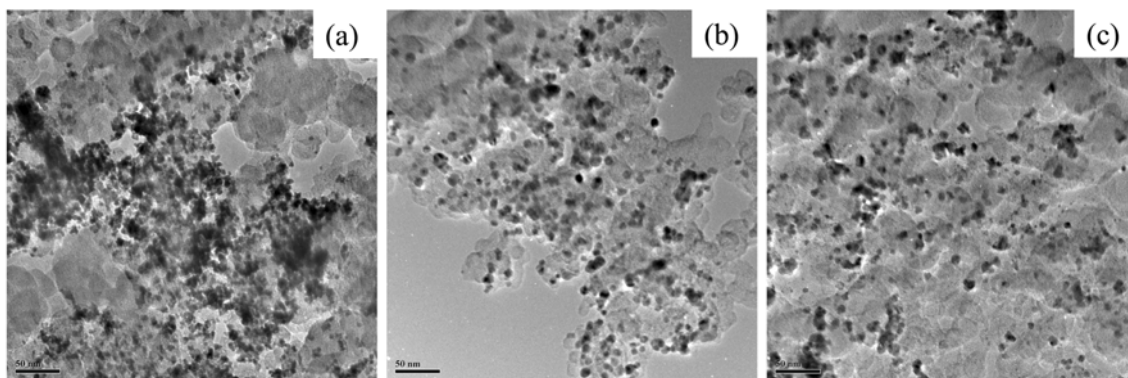


Fig. 2. TEM images of (a) Pt/C, (b) Pd/C and (c) PdPt/C catalysts (Scale bar: 50 nm).

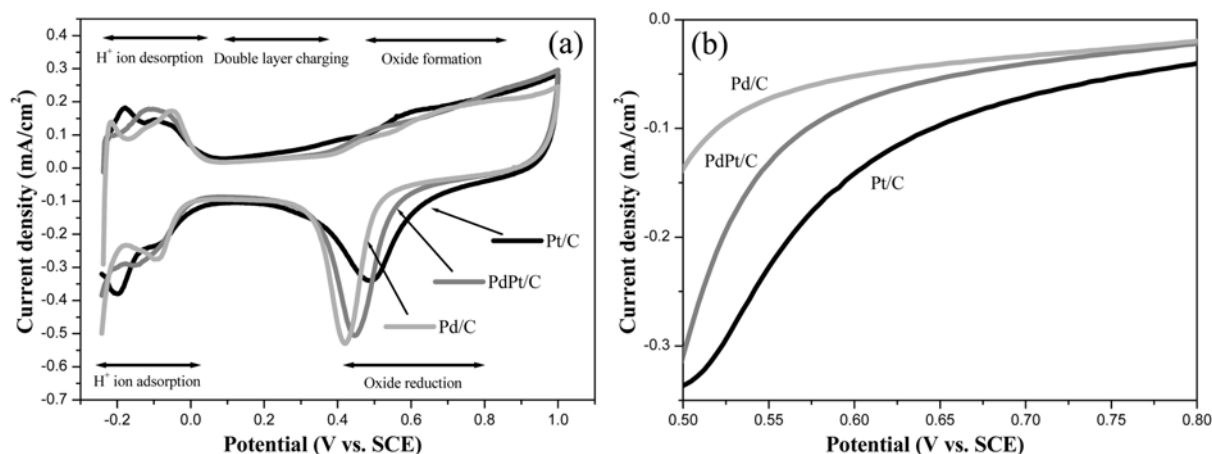


Fig. 3. (a) Cyclic voltammograms of the prepared catalysts and (b) voltammograms in the oxygen reduction region in 0.1 M  $\text{HClO}_4$ , at a scan rate of 20 mV/s.

(CVs) of the prepared Pt/C, Pd/C and PdPt/C catalysts. The CV of Pt/C catalyst exhibits the typical proton ion electro-adsorption/desorption, double-layer charging current, Pt oxide formation and oxygen reduction region. CVs of Pd/C and PdPt/C were similar to that of Pt/C. The Pd/C electrocatalyst exhibits hydrogen peaks below 0 V, which are caused by desorption of hydrogen ions on the surface of the Pd particle and dissolution of the adsorbed hydrogen into the bulk of the Pd particle. In the ORR region [Fig. 3(b)], the PdPt/C catalyst exhibited lower overpotential in oxide reduction than the Pd/C catalyst. It should be noted that the ORR kinetics of Pd catalysts was enhanced by the addition of a small amount of Pt as seen Fig. 3(b).

In order to evaluate catalytic activities of the prepared catalysts in ORR, linear sweep voltammetry was conducted at a scan rate of 5 mV/s using a rotating disk electrode (RDE). Fig. 4 shows the representative polarization curve of Pt/C and polarization curves of Pt/C, Pd/C and PdPt/C in terms of onset potential (inset figure) for ORR at 1,500 rpm in an oxygen-saturated 0.1 M  $\text{HClO}_4$  solution. In the linear sweep voltammogram, the polarization curve exhibited three regions: Tafel region, mixed diffusion-kinetics control region and diffusion-control region. The limiting current was observed in the diffusion control region (below 0.4 V) indicating that the diffusion process becomes the dominant step in the electrocatalytic reaction. Compared to Pt/C catalysts, two Pd-based catalysts had lower onset

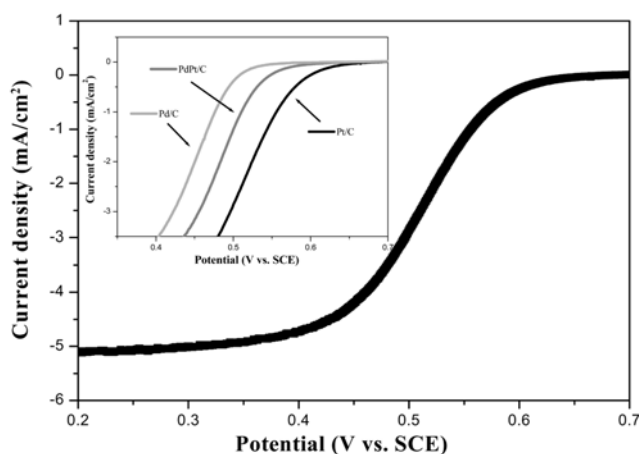


Fig. 4. Representative linear sweep voltammograms of the Pt/C catalysts and ORR polarization curves of the prepared catalysts in terms of onset potential in oxygen-saturated 0.1 M  $\text{HClO}_4$  at a scan rate of 5 mV/s and with a rotating speed of 1,500 rpm.

potential in oxygen reduction (inset in Fig. 4). This indicates that overpotentials of Pd-based catalysts are higher than that of the Pt/C catalyst in oxygen reduction. In terms of onset potential for oxygen

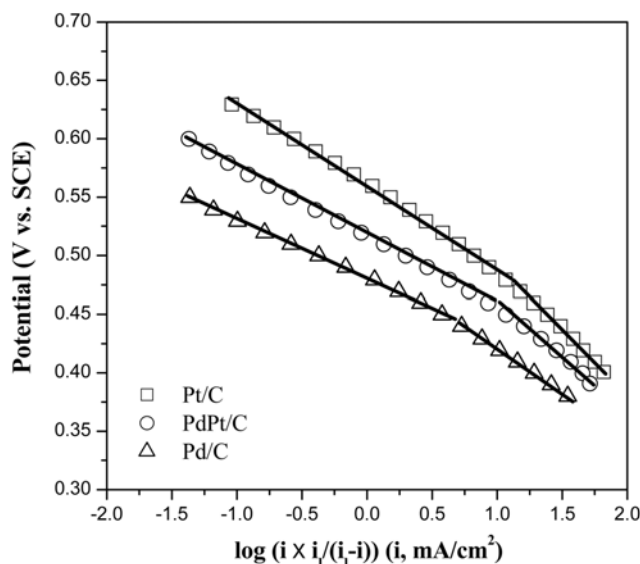


Fig. 5. Mass-transport corrected Tafel plots for the oxygen reduction reaction of the prepared catalysts in oxygen-saturated 0.1 M HClO<sub>4</sub> with a rotating speed of 1,500 rpm.

reduction, the PdPt/C catalyst exhibited lower cathodic potential than the Pd/C catalyst. Consistent with cyclic voltammetry results, ORR activity of the PdPt/C catalyst was enhanced by the addition of a small amount of Pt resulting in the formation PdPt alloy.

Further characterization of electrocatalytic activities of the prepared Pt/C, Pd/C and PdPt/C was carried out with Tafel plots. Fig. 5 shows mass transport-corrected Tafel plots of the Pt/C, Pd/C and PdPt/C catalysts for ORR by plotting potential vs.  $i \times i_L / (i_L - i)$ , where  $i_L$  is the diffusion-limiting current. Two different Tafel linear regions were observed for ORR in all electrocatalysts, with slopes near 60 and 120 mV/dec at low current density region and high current density region, respectively. This indicates that ORR mechanisms of the Pt/C, Pd/C and PdPt/C catalysts are similar. For platinum and other metal electrodes, the oxygen reduction mechanism in acidic

solution has been sufficiently discussed in previous works [29-31]. The above values of slope have been explained in terms of the coverage of adsorbed oxygen with the Temkin isotherm at low overpotential and the Langmuir isotherm at higher overpotential [32]. Based on Tafel plots, Pt/C exhibited the highest ORR activity at all overpotential regions. Although PdPt/C had slightly lower ORR activity than Pt/C, the addition of a small amount of Pt significantly enhanced the activity, compared to pure Pd/C.

Fig. 6 shows the oxygen reduction voltammograms of the prepared Pt/C, Pd/C and PdPt/C catalysts in oxygen-saturated 0.1 M HClO<sub>4</sub> solution containing 0.5 M methanol. Generally, small amounts of active Pt sites result in less methanol activity and higher methanol tolerance. In order to compare the methanol tolerance of PdPt/C catalysts per amount of Pt, the 3.5 wt% Pt/C, which has the same amount of Pt on carbon support with PdPt/C (5 : 1), was prepared and ORR activity was investigated. The Pt/C catalyst exhibited high methanol electro-oxidation peak at 0.52 V during the cathodic sweep. Pt/C has high overpotential for the ORR due to the simultaneous reaction of the ORR and the methanol oxidation reaction (MOR). 3.5 wt% Pt/C catalyst showed also small methanol oxidation peak (Fig. 6 (insert)). On the other hand, no such current peak was observed on Pd/C catalyst, which indicates that Pd/C has no significant catalytic activity for methanol electro-oxidation. As compared to linear sweep voltammograms in 0.1 M HClO<sub>4</sub> (Fig. 4), the Pd/C exhibited almost similar voltammograms in 0.1 M HClO<sub>4</sub> containing 0.5 M methanol as shown in Fig. 6. The PdPt/C catalyst showed similar linear sweep voltammograms during the cathodic sweep in oxygen-saturated 0.1 M HClO<sub>4</sub> solution containing methanol. As compared to Pd/C catalyst, the onset potential of PdPt/C was enhanced to lower cathodic potential, indicating that the ORR activity was enhanced. In addition, no MOR-related peak was observed in linear sweep voltammograms, indicating that the PdPt/C catalyst has methanol-tolerant characteristics because of alloying Pd with Pt. Thus PdPt/C catalyst showed enhanced activity in terms of onset potential and tolerance toward methanol oxidation.

## CONCLUSIONS

Pd-based alloy catalyst with small Pt content was prepared by sodium borohydride reduction and the ORR activity was investigated in acidic electrolyte both with and without alcohol. Compared to pure Pd/C catalyst, the ORR activity of PdPt/C catalyst was significantly enhanced in terms of onset potential. It originated from the formation of alloy structure between Pd and Pt by addition of a small amount of active Pt. The PdPt/C catalyst also has a selective activity toward oxygen electro-reduction while maintaining methanol tolerance. From the experimental results, we concluded that the selective and enhanced activity is the result of the formation of PdPt alloy. Therefore, PdPt/C catalyst described herein is a potential candidate for the electrode catalyst in direct methanol fuel cells.

## ACKNOWLEDGMENTS

This work was supported by grant No. (R01-2006-000-10239-0) from the Basic Research Program of the Korea Science & Engineering Foundation and J. Yi thanks for SNU Engineering Research Institute. J. Yi is grateful for an SBS Foundation grant and wishes

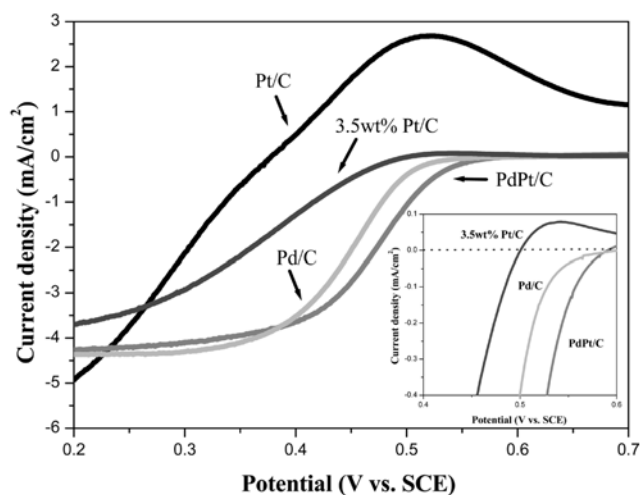


Fig. 6. Linear sweep voltammograms of the prepared catalysts in oxygen-saturated 0.1 M HClO<sub>4</sub>+0.5 M MeOH at a scan rate of 5 mV/s with a rotating speed of 1,500 rpm.

to thank R. N. Zare, Stanford University, for his hospitality while this manuscript was prepared during his sabbatical.

## REFERENCES

1. Z. Liu, L. M. Gan, L. Hong, W. Chen and J. Y. Lee, *Power Source*, **139**, 73 (2005).
2. T. Matsumoto, T. Komatsu, K. Arai, T. Yamazaki, M. Kijima, H. Shimizu, Y. Takasawa and J. Nakamura, *Chem. Comm.*, 840 (2004).
3. H. Wang and I.-M. Hsing, *Electrochim. Acta*, **47**, 2981 (2002).
4. J. S. Kim, J. K. Yu, H. S. Lee, J. Y. Kim, Y. C. Kim, J. H. Han, I. H. Oh and Y. W. Rhee, *Korean J. Chem. Eng.*, **22**, 661 (2005).
5. T.-H. Yang, G. Park, P. Paugazhendhi, W.-Y. Lee and C. S. Kim, *Korean J. Chem. Eng.*, **19**, 417 (2002).
6. S. Lee, D. Kim, S. Lee, S. T. Chung and H. Y. Ha, *Korean J. Chem. Eng.*, **22**, 406 (2005).
7. C. Park, S. J. Lee, S.-A. Lee and H. Lee, *Korean J. Chem. Eng.*, **22**, 214 (2005).
8. W. Hawut, M. Hunson and K. Pruksathorn, *Korean J. Chem. Eng.*, **23**, 255 (2006).
9. H. Li, Q. Xin, W. Li, Z. Zhou, L. Jiang, S. Yang and G. Sun, *Chem. Comm.*, 2776 (2004).
10. H. Zhong, H. Zhang, Y. Liang, J. Zhang, M. Wang and X. Wang, *J. Power Sources*, **164**, 572 (2007).
11. K. Lee, L. Zhang and J. Zhang, *J. Power Sources*, **165**, 108 (2007).
12. C. Xu, P. Shen and Y. Liu, *J. Power Sources*, **164**, 527 (2007).
13. J. Fourmier, G. Faubert, J. Y. Tilquin, R. Cote, D. Guay and J. P. Dodelet, *J. Electrochem. Soc.*, **144**, 145 (1997).
14. S. Ye, A. Vijn and L. Dao, *J. Electroanal. Chem.*, **415**, 115 (1996).
15. N. Alonso-Vante and H. Tributsch, *Nature*, **323**, 431 (1986).
16. N. Alonso-Vante, W. Jaegermann, H. Tributsch, W. Honle and K. Yvon, *J. Am. Chem. Soc.*, **109**, 3251 (1987).
17. R. W. Reeve, P. A. Christensen, A. J. Dickinson, A. Hamnett and K. Scott, *Electrochim. Acta*, **145**, 3463 (2000).
18. M. C. Martins Alves, J. P. Melet, D. Guay, M. Ladouceur and G. Tourillon, *J. Phys. Chem.*, **96**, 10898 (1992).
19. L. T. Weng, P. Bertrand, G. Lalande, D. Guay and J. P. Dodelet, *Appl. Surf. Sci.*, **84**, 9 (1995).
20. L. Zhang, J. Zhang, D. P. Wilkison and H. Wang, *J. Power Sources*, **156**, 171 (2006).
21. K. Lee, J. Zhang, H. Wang and D. P. Wilkison, *J. Appl. Electrochem.*, **36**, 507 (2006).
22. A. Capon and R. Parsons, *J. Electroanal. Chem.*, **44**, 239 (1973).
23. C. Lamy, *Electrochim. Acta*, **29**, 1581 (1984).
24. O. Savadogo, K. Lee, K. Oishi, S. Misushima, N. Kamiya and K. I. Ota, *Electrochem. Comm.*, **6**, 105 (2004).
25. J. L. Fernandez, V. Raghuvier, A. Manthiram and A. J. Bard, *J. Am. Chem. Soc.*, **38**, 127 (2005).
26. V. Raghuvier, A. Manthiram and A. J. Bard, *J. Phys. Chem. B*, **48**, 109 (2005).
27. Y.-H. Cho, B. Choi, Y.-H. Cho, H.-S. Park and Y.-E. Sung, *Electrochem. Comm.*, **9**, 378 (2007).
28. K. Kinoshita, *Electrochemical oxygen technology*, John Wiley & Sons Inc (1992).
29. B. Sepa, M. Vojnovic and A. Damjanovic, *Electrochim. Acta*, **26**, 781 (1981).
30. Q. Huang, H. Yang, Y. Tang, T. Lu and D. L. Akins, *Electrochem. Comm.*, **8**, 1220 (2006).
31. L. Zhang, K. Lee and J. Zhang, *Electrochim. Acta*, **52**, 3088 (2007).
32. E. Antolini, J. R. C. Salgado, L. G. R. A. Santos, G. Garcia, E. A. Ticianelli, E. Pastor and E. R. Gonzalez, *J. Appl. Electrochem.*, **36**, 355 (2006).
33. M. R. Tarasevich, A. E. Chalykh, V. A. Bogdanovskaya, L. N. Kuznetsova, N. A. Kapustina, B. N. Effremov, M. R. Ehrenburg and L. A. Reznikova, *Electrochim. Acta*, **51**, 4455 (2006).
34. K. Lee, O. Savadogo, A. Ishihara, S. Mitsushima, N. Kamiya and K. Ota, *J. Electrochem. Soc.*, **153**, A20 (2006).